



# Assessment of groundwater recharge and connectivity with surface water in a mountainous watershed using natural tracers in Daejeon, Korea

Hanna Choi<sup>1</sup> · Chung-Mo Lee<sup>2</sup> · Hui Je Jo<sup>3</sup> · Byoung Ohan Shim<sup>1</sup>

Received: 30 March 2023 / Accepted: 23 September 2023 / Published online: 21 October 2023  
© The Author(s) 2023

## Abstract

The water supply from headwater streams in mountainous regions is considered an important source for sustaining both water quality and quantity in lowland areas. The Korean terrain is characterized by mountainous regions, the hydrological environment is significantly impacted by seasonal weather conditions. This study focused on investigating the hydrochemistry and isotopic composition of groundwater and surface water to identify hydrological connectivity within a mountainous watershed area in Daejeon, Korea. The estimated recharge rate using water budget methods suggests that approximately 20% of the total precipitation contributes to groundwater recharge in this site. The  $\delta^{18}\text{O}$ – $\delta^2\text{H}$  values of the water samples indicate a meteoric water source for groundwater recharge, while the isotope composition of surface water reveals altitude effects, implying that groundwater recharges at a higher altitude region. Additionally, water revealed altitude effects suggesting that the groundwater was inferred to recharge at a higher altitude region. The hydrochemical conservative components ( $^{87}\text{Sr}/^{86}\text{Sr}$  ratio and  $\text{Cl}^-$ ) indicate that this watershed undergoes temporary similar water–rock interactions along its flow path, but it is also impacted by anthropogenic contaminants from the surrounding public area. The results of the three-component endmember mixing analysis demonstrate that groundwater is predominantly influenced by surface water, indicating a close interrelationship among various water bodies in mountain hydrology. These findings provide a comprehensive approach to water resource management by combining recharge rate estimation and the assessment of water body connectivity using natural tracers.

**Keywords** Mountainous watershed · Groundwater recharge · Isotope analysis · Endmember mixing analysis (EMMA)

## Introduction

Climate change is associated with the incidence of extreme weather events which have led to a gradual diminution in the available water resources (IPCC 2021). As urbanization accelerates, there is a prevailing consensus that the issue of water scarcity is gradually becoming a reality (Zou et al. 2019; Munia et al. 2020). Especially, mountain regions

are encountered to alter hydrological regimes by socio-economic factors, such as deforestation, excessive pumping for agriculture, or domestic usage. The water supply from headwater streams serves as an important source for lowland areas, and thus, the degradation of water contribution from mountainous watershed will have negative impacts on downstream water quality and quantity (Somers and McKenzie 2020; Yifru et al. 2022). Approximately 70% of South Korea's total land area is comprised of mountainous terrain (NGII 2016), and the hydrological environment is significantly influenced by seasonal weather conditions. Recent studies have reported the substantial capacity of mountainous groundwater storage which is maintaining and buffering the streamflow including dry season (Jang et al. 2015; Jung et al. 2019; Somers and McKenzie 2020). Since there is a close interrelationship between surface water and groundwater in mountain hydrology, it is important to interpret factors, such as recharge rate estimation, background water quality, and pollution sources.

✉ Byoung Ohan Shim  
boshim@kigam.re.kr

<sup>1</sup> Climate Change Response Division, Korea Institute of Geoscience and Mineral Resources, Daejeon 34132, Republic of Korea

<sup>2</sup> Department of Geological Sciences, Pusan National University, Busan 46241, Republic of Korea

<sup>3</sup> Geology and Space Division, Korea Institute of Geoscience and Mineral Resources, Daejeon 34132, Republic of Korea

There are various existing groundwater recharge models that consider spatiotemporal variability owing to climatic conditions, land use, soil type, and hydrogeological heterogeneity (Scanlon et al. 2005; Anuraga et al. 2006; Owuor et al. 2016). The developed models were adapted to groundwater recharge estimation via water balance measurements, contaminant movement, numerical models, lysimetric and tracer tests, and Darcian flux calculations (Aboukhaled et al. 1982; Gee and Hillel 1988; Xu and Chen 2005; Wu et al. 2016). For a regional-scale watershed or above area, the water budget method is cost-effective and easy to apply to estimate groundwater recharge (Manghi et al. 2009). Owing to the convenience of applying meteorological data and satellite images with geographical information systems (GIS), it has become possible to analyze water balance accurately over a wide area (Gonzalez et al. 2016). Based on the methods of previous researchers, this study adapted the water budget method introduced by Scanlon et al. (2002) to evaluate groundwater recharge using meteorological data and direct runoff data from the study area. The recent precipitation trend in South Korea is more biased in the summer season than in previous years according to climate change (Kang et al. 2018), which would influence water circulation systems and modify the recharge rate (Havril et al. 2018).

Many research have been conducted in Korea to investigate the connectivity of water bodies using conservative chemical or biological indicators, and these works have demonstrated the flow system or mixing ratio within mountain watersheds (Yun et al. 2003; Jung et al. 2019; Choi et al. 2020; Kim et al. 2020). However, regional-scale studies have not provided specific hydrochemical information within the target area through intensive sampling, owing to the spatial representative limitations. In comparison, local-scale studies primarily focus on water bodies within the target basin, necessitating an understanding of hydrological processes within the broader river system. Therefore, this study carried out local-scale study on the mountainous watershed and regional connectivity between groundwater and surface water considering higher order streams associated with target watersheds. The aims of this study were to estimate the recharge rate based on hydraulic water budget method; to identify the factors controlling hydrochemical properties of water bodies using chemical and isotopic variables; and to identify pollution sources and quantify determinants fluxes considering both groundwater and surface water. Based on these results, we will discuss recharge process and water quality determination factors in this mountainous watershed, and connectivity of surface water and groundwater and their impacts on the higher order stream.

## Site description

Gapcheon River has a watershed area of about 648.9 km<sup>2</sup>, and the total channel extension is 73.7 km. Figure 1A presents the entire Gapcheon watershed area, with the surface elevation data in green-colored gradation representing the area of Daejeon Metropolitan City. The red-colored boundary represents the Tandongcheon watershed area. The upstream of Gapcheon River (southern part of N1) is connected to the provincial park as a nature conservation area, and it was reported to have the surface water and groundwater quality characteristics of mountainous areas (Hur et al. 2008; Hur and Cho 2012; Jung et al. 2019). The Gapcheon River exhibits excellent water quality at upstream, but total nitrogen (TN), total phosphorus (TP), and phytoplankton biomass (Chlorophyll-*a*) deteriorated from upstream to downstream during the dry season indicating distinct spatial contamination levels (Lee et al. 2006). Jang et al. (2019) reported that the river meets appropriate water quality standards for biochemical oxygen demand (BOD), chemical oxygen demand (COD), and total organic carbon (TOC) indices before flowing into Daejeon City. The N1, N2, and N3 points in Fig. 1A are national water quality monitoring sites conducted once a month by Daejeon City. Urban facilities are being developed from the N1 point, and this site receives effluent from a reservoir used for agricultural purposes (Jang et al. 2019). The N2 is located in the center of the new town in Daejeon City, and thus, the impact of the inflow from non-point pollution sources would be immediately reflected in the water quality. The N3 is an observation point located approximately 2.5 km downstream from the effluent of a large-scale municipal wastewater treatment plant (WWTP) in Daejeon City.

Tandongcheon stream is one of the tributaries flowing into the Gapcheon River through the center of Daejeon City and converging just before the WWTP discharge point. The Tandongcheon watershed area (approximately 2.9 km<sup>2</sup>), which is located in the Yuseong-gu region of Daejeon Metropolitan City (36° 21' 27"–36° 25' 57" N, 127° 19' 11"–127° 24' 08" E), is classified into sub-watershed according to Agriinfo (2018). This area is surrounded by mountains on three sides, with the exception being the Gapcheon River in the south, and the Tandongcheon Stream flows from the north to the south along the watershed center. At the upstream, there are military installations and corresponding sewage treatment facilities. Moreover, it has been reported that the stream contamination is caused by non-point source pollutants originating from residential and aged sewage facilities located in the midstream (Yin and Seo 2013). In contrast to Gapcheon National River, there is no long-term water quality data of

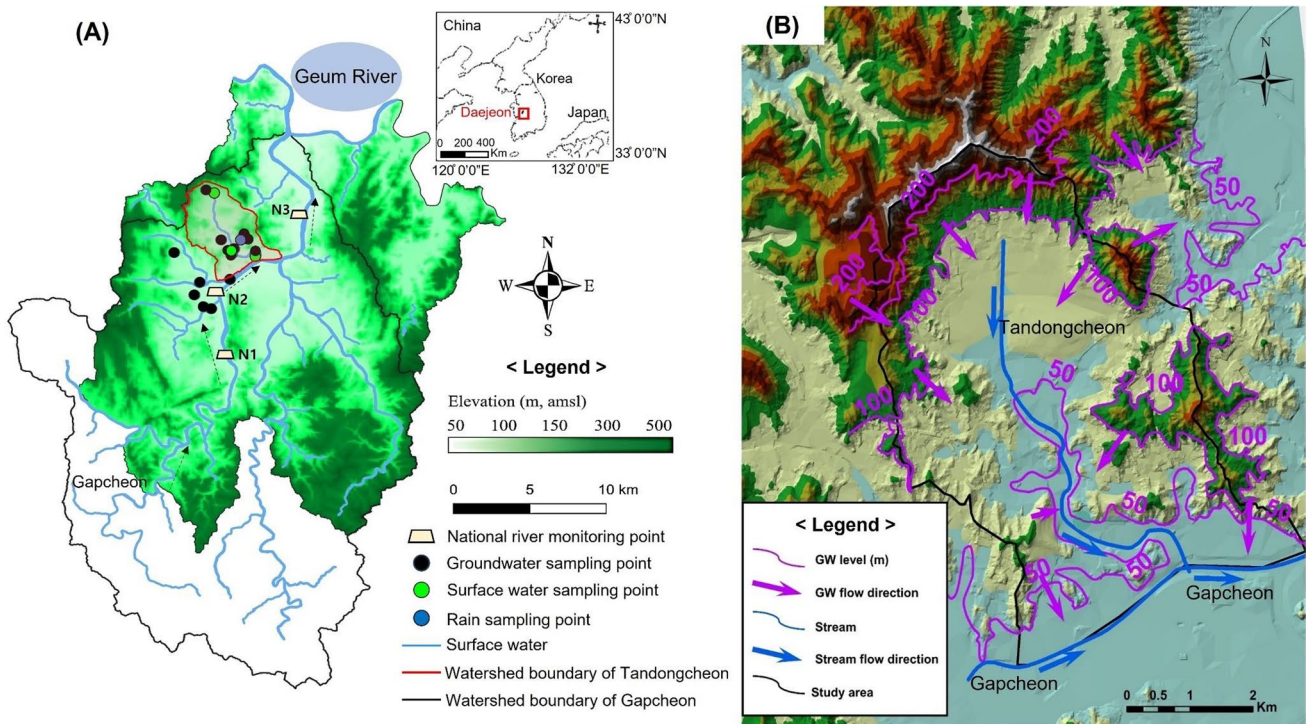


**Fig. 1** Gapcheon River watershed area and the boundary of Daejeon Metropolitan City. **A** The red-colored area represents the Tandongcheon sub-watershed, and **B** the groundwater level and flow direction of the Tandongcheon

Tandongcheon stream due to the absence of facilities for continuous water quality and quantity observation.

Figure 1B shows the groundwater level and flow direction based on the groundwater information provided by the Korean National Groundwater Information Center ([www.gims.go.kr](http://www.gims.go.kr)). We drew the flow direction map of groundwater and surface water with Golden Software Surfer 17. It seemed that the local groundwater discharges into the Tandongcheon Stream, while regional groundwater discharges into the direction of the Gapcheon River. The groundwater discharge and surface water flow direction are closely related to the regional topographic gradient.

The watershed is geologically located in the central part of the Okcheon belt (Fig. 2). Precambrian metamorphic rocks, Paleozoic metasedimentary rocks, and Jurassic granitoids are exposed in the Yuseong area (Lee et al. 2021). Jurassic plutons predominantly comprise peraluminous two-mica granites with minor diorite. These plutons intruded Precambrian basement rocks and Paleozoic metasediments and are considered to have originated from the partial melting of juxtaposed allochthonous terranes (Jo et al. 2018). Hwang et al. (2013) proved that hydrothermally altered and weathered granitic dykes and the body are the primary source materials of U in groundwater.

## Materials and methods

### Water budget estimation

The water budget estimate is calculated under the assumption that water balance is maintained by the amount of precipitation, direct runoff, evapotranspiration, and groundwater recharge in the watershed. Based on it, the hydraulic water budget method is expressed as follows:

$$I = P - DR - ET, \tag{1}$$

where I is the groundwater recharge, P is the precipitation, DR is the direct runoff, and ET is the evapotranspiration. Direct runoff varies with the hydraulic features of the surface, which frequently change owing to urbanization or forest development. To calculate groundwater recharge, it is necessary to use data related to groundwater, such as meteorological and hydraulic properties, vegetation, soil, and geological features. However, it is difficult to reflect hydraulic features because of their rapidly changing nature, and groundwater recharge is usually indirectly calculated using previous methods, such as aerodynamic, water balance, and empirical equations.

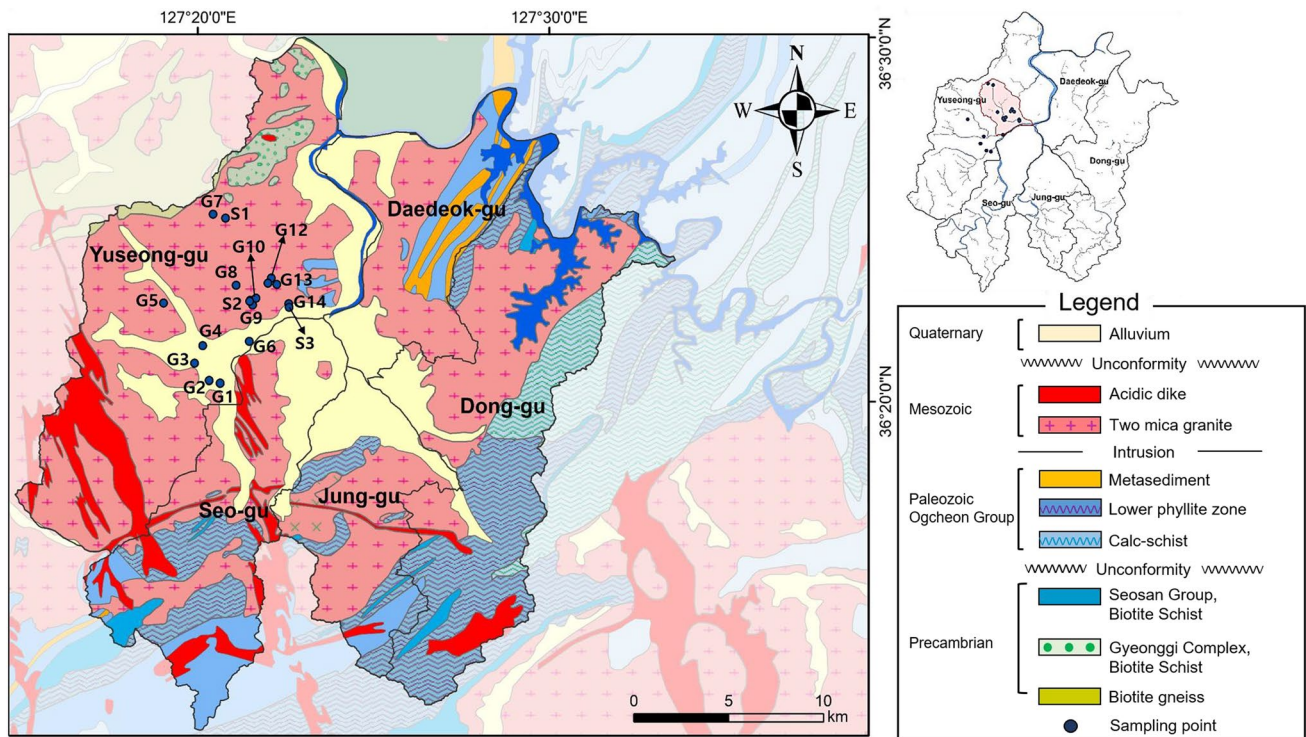


Fig. 2 Geological setting and sampling points of Daejeon Metropolitan City

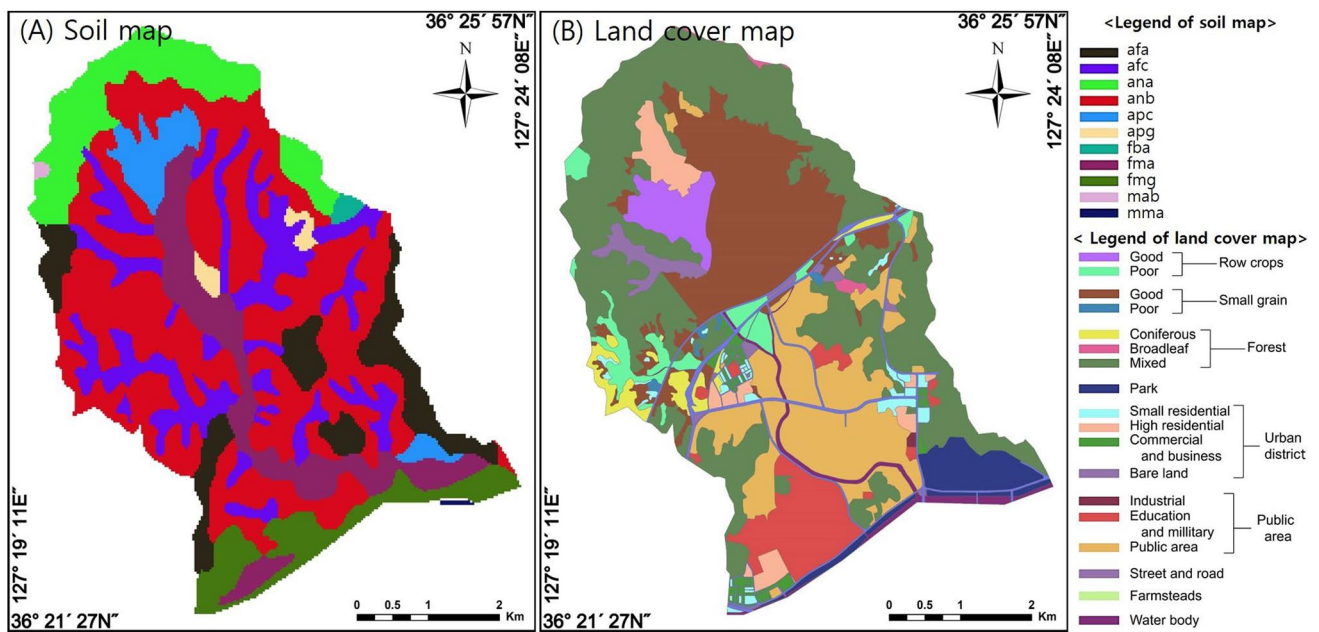


Fig. 3 A Soil map and B land-cover map of the study site for the GIS analysis

In the GIS analysis, the adapted soil map is a 1:50,000 scale map developed by the Water Resources Management Information System funded by the Ministry of Land,

Transport, and Maritime Affairs (Fig. 3A). The land-cover map of this study area has a scale of 1:25,000 and was provided by the National Spatial Data Infrastructure Portal (Fig. 3B).

**Table 1** A Land-cover properties and B hydrological soil group classification

(A) Land-use property			
Description	Treatment or practice	Area (km <sup>2</sup> )	
Row crops	Good	0.86	
	Poor	0.94	
Small grain	Good	5.05	
	Poor	0.09	
Forest	Coniferous	0.54	
	Broadleaf	0.09	
	Mixed	10.18	
Urban district	Residential districts	0.92	
	Commercial and business	0.34	
	Open space	0.56	
	Bare land	1.11	
Public area	Industrial	0.02	
	Public area	4.43	
	Education and military	2.28	
Street and road	–	0.99	
Farmsteads	–	<0.01	
Water body	–	0.47	
(B) Hydrologic soil group			
Type	Soil series	Permeability	Soil texture
A	afa, afc, anb, fba, fmg	High	Chiefly sands and gravels
B	apc, apg, mab, mma	Moderate	Moderately fine and coarse
C	ana	Slow	Moderately fine
D	fma	Very slow	Silty and clay

The land-cover map was classified into seven major categories (row crops, small grain, forest, urban district, public area, street and road, and water body in Table 1A). The soil map was classified into 11 categories (afa, afc, ana, anb, apc, apg, fba, fma, fmg, mab, and mma of soil symbols in Table 1B) and respective minor categories. The hydrological soil groups were classified according to the hydrologic soil type obtained from a 1:50,000 scale soil map provided by the National Institute of Agricultural Science and Technology.

### FAO-56 FM method

The FAO developed the way to estimate reference evapotranspiration based on crop coefficients (Kc) and the revised and supplemented FAO-56 PM method was suggested by Allen et al. (1998). This study suggested atmospheric temperature, humidity, wind speed, and radiation as the most important

data to collect out of the factors influencing reference evapotranspiration. From January 1990 to May 2020, this study collected minimum temperature (°C), maximum temperature (°C), average temperature (°C), relative humidity (%), average wind speed (m/s), duration of sunshine (h), precipitation (mm), atmospheric pressure (hpa), station elevation (EL m), and radiation (MJ/m<sup>2</sup>/day) data at the Daejeon weather station (N36°37'19.8", E127°37'21.1"), which is the closest to the study area.

With regard to the FAO-56 FM equation, surface Albedo of the places where water is amply supplied is 0.23 and reference evapotranspiration is estimated by setting 0.12 m-high grass as standard crop. The equation estimating daily reference evapotranspiration is the following (Allen et al. 1998).

$$ET_0 = \frac{0.408\Delta(R_n - G) + \gamma \frac{900}{T+273} u_2(e_s - e_a)}{\Delta + \gamma(1 + 0.34u_2)}, \tag{2}$$

where the abbreviations mean the following,  $ET_0$  reference evapotranspiration (mm/day),  $Rn$  net radiation ( $\text{MJ}/\text{m}^2/\text{day}$ ),  $G$  soil heat flux ( $\text{MJ}/\text{m}^2/\text{day}$ ),  $\gamma$  psychrometric constant ( $\text{kPa}/^\circ\text{C}$ ),  $\Delta$ : slope vapor pressure curve ( $\text{kPa}/^\circ\text{C}$ ),  $e_s$  saturation vapor pressure (kPa),  $e_a$  actual vapor pressure (kPa),  $T$  mean daily air temperature at 2 m height ( $^\circ\text{C}$ ), and  $u_2$  wind speed at 2 m height (m/s). The factors related to solar radiation and maximum possible duration of sunshine (N) applied the north latitude 36 degrees of the weather station which have been provided as empirical equation in the FAO-56. In this study, crop coefficient was applied to grass with a height of 0.12 m.

## SCS-CN method

The basic concept equation of the SCS-CN method, which the method of calculating direct runoff is taking place due to rainfall, is expressed as Eq. (3). The time step was calculated on a daily basis, the values were summed on a yearly, and presented the average value for 30 years

$$\text{DR} = \frac{(P - I_a)^2}{P - I_a + S} \text{ for } P > I_a, \quad (3)$$

$$\text{DR} = 0 \text{ for } P \leq I_a.$$

Here,  $P$  is total rainfall,  $I_a$  is initial abstraction,  $\text{DR}$  is direct runoff, and  $S$  is potential maximum retention.  $I_a = 0.2S$  suggested by Ponce and Hawkins (1996) was used for this calculation and  $S$  value was derived using runoff curve number after using antecedent soil moisture condition suggested by the Soil Conservation Service. When applying antecedent moisture condition (AMC) after considering Korea's climate of intensive rain in summer, calculations have been done by dividing into growing season (June–September) and dormant season (October–May). Accumulated 5-day antecedent rainfall during dormant season is  $\text{AMC-I} < 12.7 \text{ mm} < \text{AMC-II} < 28.0 \text{ mm} < \text{AMC-III}$  and that of growing season is  $\text{AMC-I} < 35.56 \text{ mm} < \text{AMC-II} < 53.34 \text{ mm} < \text{AMC-III}$ . Initial soil condition is classified into AMC-I, AMC-II, and AMC-III based on accumulated 5 day antecedent rainfall and respective AMCs are calculated as CN-I, CN-II, and CN-III. This process is Eq. (4)

$$\begin{aligned} \text{CN(I)} &= \frac{4.2\text{CN(II)}}{10 - 0.058\text{CN(II)}}, \\ \text{CN(III)} &= \frac{23\text{CN(II)}}{10 + 0.13\text{CN(II)}}. \end{aligned} \quad (4)$$

**Table 2** Curve numbers (CN) for land covers

Description	Treatment or practice	Hydrologic soil group			
		A	B	C	D
Row crops	Good	78	78	78	78
	Poor	78	78	78	78
Small grain	Good	63	78	85	89
	Poor	62	73	80	83
Forest	Coniferous	46	68	79	86
	Broadleaf	47	67	78	85
	Mixed	47	68	79	86
Urban district	Residential districts	48	67	78	83
	Commercial and business	89	92	94	95
	Open space	77	86	91	94
	Bare land	77	86	91	94
Public area	Industrial	81	88	91	93
	Public area	89	92	94	95
	Education and military	89	92	94	95
Street and road	–	97	91	93	94
Farmsteads	–	44	66	77	83
Water body	–	100	100	100	100

AMC varies according to type of soil, vegetation, and land cover. The previously mentioned contents are Eq. (5) in a nutshell

$$S = \frac{25,400}{\text{CN}} - 254. \quad (5)$$

CN is determined according to hydraulic soil group (Table 1) and land cover (Table 2) of the study area. Hydrologic soil group is classified into four types based on features. Direct runoff increases as infiltration rate decreases as it progresses from A to D.

## Sample collection and analysis

Groundwater and surface water samples were collected in June 2021, and precipitation samples were collected in March (R1) and in June (R2 and R3) of 2021. Figure 4 presents the sampling points and the flow direction of the surface water in the study area. The precipitation samples (R1 to R3) were collected from same site where the central grassland at the Korea Institute of Geoscience and Mineral Resources (KIGAM) site, represented by the blue dots (R1) in Fig. 4, and surface water sample (S1) was collected from uppermost site of the Tandongcheon Stream.

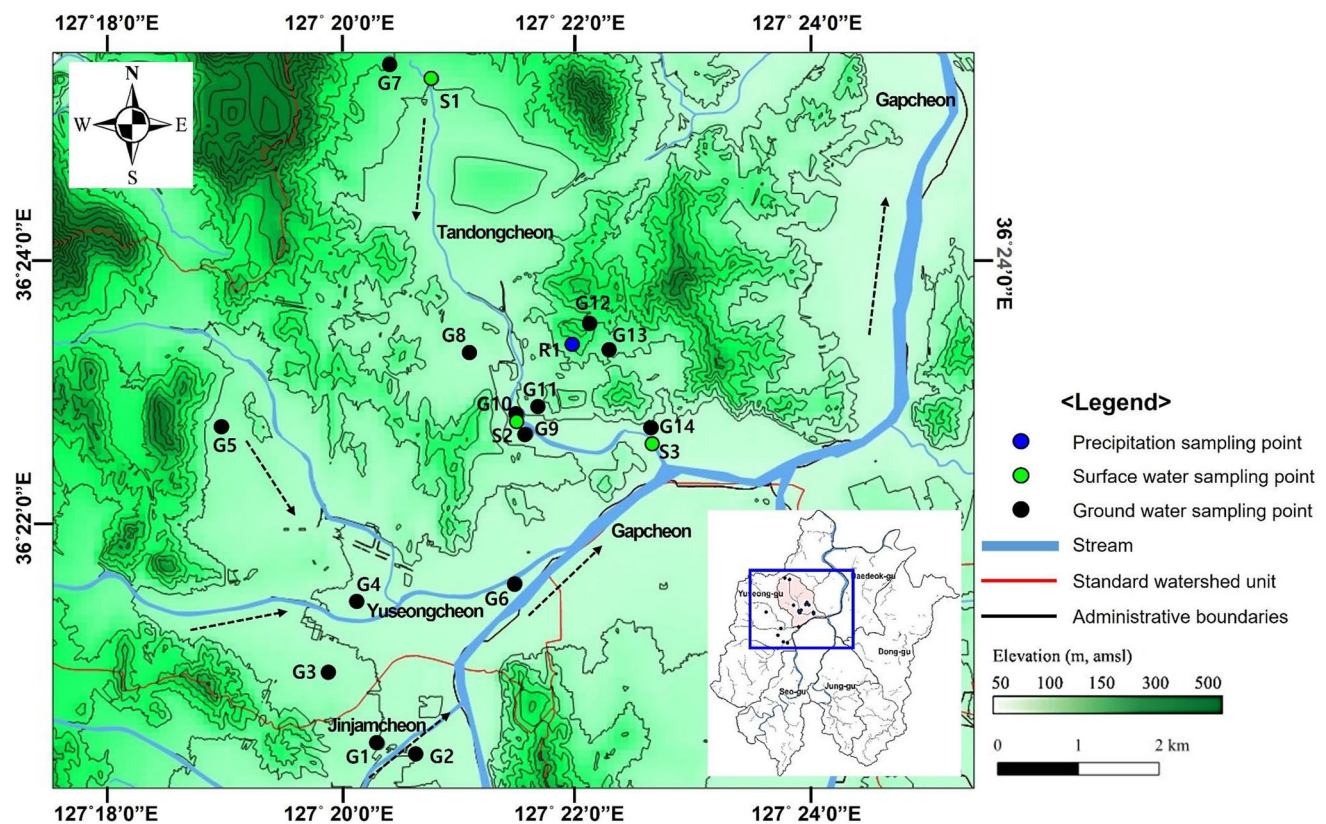


Fig. 4 Sampling points of discharge and water quality in the Gapcheon River tributaries

The midstream water (S2) and downstream water (S3) was collected from the location just before the confluence of the Gapcheon River.

Water temperature, pH, electrical conductivity (EC), and dissolved oxygen (DO) were measured in the field using a multiparameter WTW (Multi 3620 IDS, Fisher Scientific); the water samples were filtered through 0.45- $\mu\text{m}$  acetate cellulose filters. The concentrations of major cations and anions ( $\text{Na}^+$ ,  $\text{K}^+$ ,  $\text{Ca}^{2+}$ ,  $\text{Mg}^{2+}$ ,  $\text{Cl}^-$ ,  $\text{SO}_4^{2-}$ ,  $\text{HCO}_3^-$ , and  $\text{NO}_3^-$ ), dissolved silica ( $\text{SiO}_2$ ), and trace elements ( $\text{Fe}^{2+}$ ,  $\text{Mn}^{2+}$ ,  $\text{Sr}^{2+}$ ,  $\text{F}^-$ , and  $\text{NO}_2^-$ ) were measured in the laboratory. Sample collection and analysis were performed based on the standard method suggested by Hounslow (2018).

Cation analysis was conducted using inductively coupled plasma spectroscopy-optimal emission spectrometry (ICP-OES, OPTIMA 7300DV, Perkin Elmer), and anion analysis was conducted using ion chromatography (IC, Dionex Aquion, Thermo Scientific). The measured ion concentrations and calculated charge balance errors had an error of less than  $\pm 10\%$ . The stable hydrogen ( $\delta^2\text{H}$ ) and oxygen ( $\delta^{18}\text{O}$ ) isotopic compositions of the water samples were measured using wavelength-scanned cavity

ring-down spectroscopy (WS-CRDS; L2120-i; Picarro) relative to the international standard V-SMOW (Vienna Standard Mean Ocean Water). The isotopic values can be expressed as a standard delta ( $\delta$ , ‰ unit) notation using V-SMOW (Clark and Fritz 1997). Strontium (Sr) separation and isotope measurements were performed in a class 1,000 clean room. The Sr isotopic ratios of 14 groundwater and 3 surface water samples were measured using thermal ionization mass spectrometry (TIMS). Detailed Sr separation procedures and TIMS techniques are described in Jo et al. (2021).

### Three-component endmember mixing analysis (EMMA)

For the mixing calculation of water bodies in Tandongcheon sub-watershed, this study deals with groundwater and surface water as an endmember using hydrochemical indicators, because this site is surrounded by mountains and there is no other inflowing stream except for Tandongcheon Stream. This method selects endmembers which show

clearly representative and discriminant properties among the samples. The three-component mixing analysis according to Crammer's rule of linear algebra as follows (Peng et al. 2016):

$$C_1f_1 + C_2f_2 + C_3f_3 = C_{\text{sample}}, \quad (6)$$

$$C'_1f_1 + C'_2f_2 + C'_3f_3 = C'_{\text{sample}}, \quad (7)$$

$$f_1 + f_2 + f_3 = 1, \quad (8)$$

where  $f_1, f_2,$  and  $f_3$  are the fractions of the three endmembers comprising the mixture; the numbers 1, 2, and 3 refer to each endmember water;  $C_1, C_2,$  and  $C_3$  are the ion concentrations components each endmember samples;  $C'_1, C'_2,$  and  $C'_3$  are the isotope ratio of each endmember samples.

## Results and discussion

### Calculation of watershed recharge

The annual average precipitation over these 30 years was 1347.29 mm, with an average of 68% of precipitation falling during the period of June–September (Fig. 5A). The average temperature and humidity were 12.72 °C and 67.87%, respectively. The monthly average wind speed and sunshine duration were 1.74 m/s and 6.14 h, respectively. Evapotranspiration over the 30 years, as calculated using the FAO-56 PM equation, was 884.32 mm, which is 65.64% of the total precipitation. In the hydrologic soil group (Table 1), Group A comprised the largest area (73.7%), followed by Group D (10.8%), Group C (10.0%), and Group B (5.0%). The final CN(II) value within the study area was obtained using CN and AMC based on the hydrologic soil group, and land cover was determined to be 70.695. Therefore, by

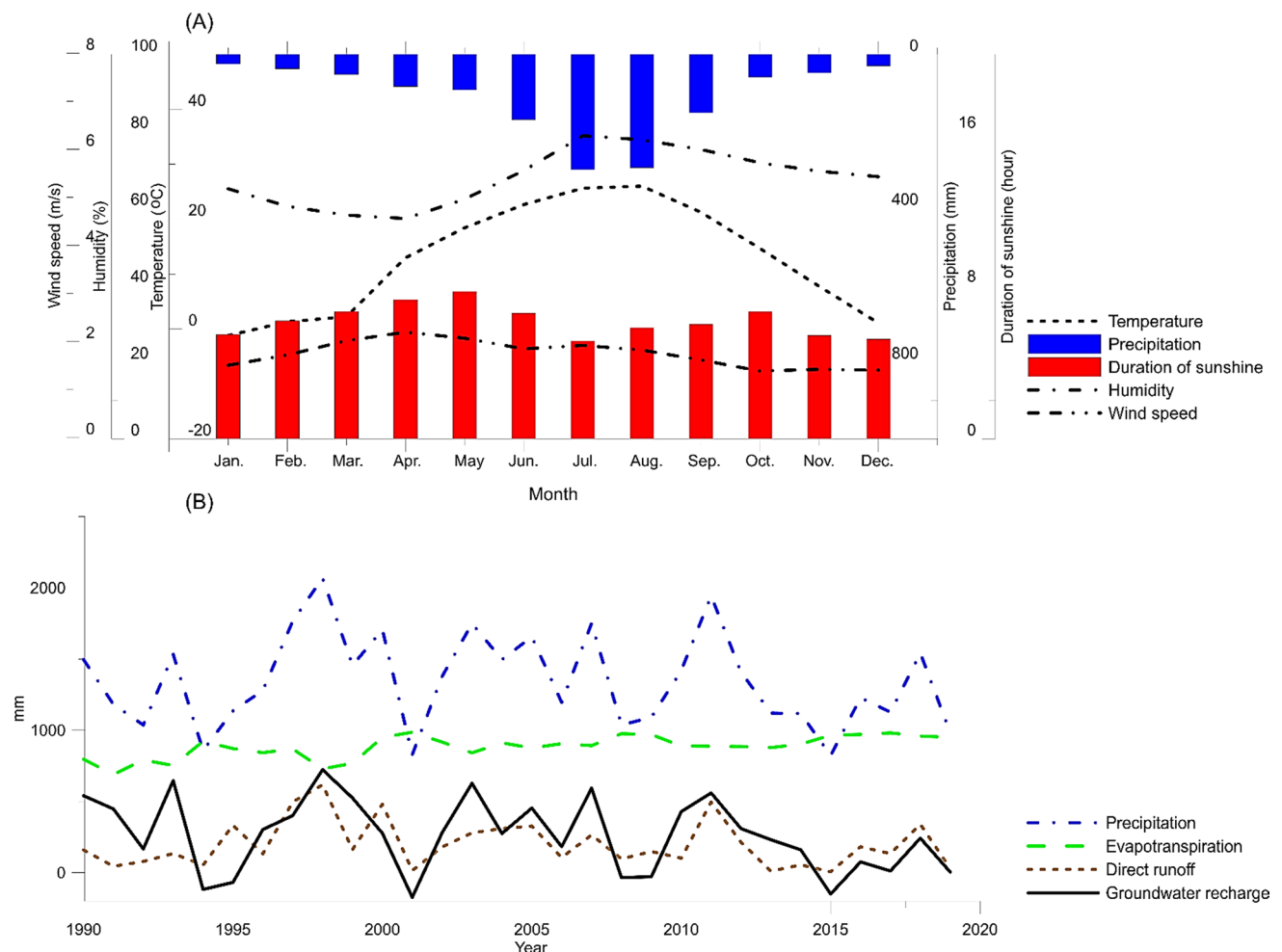


**Fig. 5** Meteorological data during 1990–2019. **A** Monthly average meteorological data and **B** annual cumulative precipitation, evapotranspiration, direct runoff, and groundwater recharge



applying the CN(II) value, the direct runoff was calculated as 199.74 mm (199 mm/year for 30 years), which was equal to 14.83% of the total precipitation (1347.29 mm). When the hydrological cycle was calculated with the water budget component, we assumed that precipitation, direct runoff, evapotranspiration, and groundwater recharge were balanced. Since the total precipitation within the study area was 1347.29 mm, evapotranspiration was 884.32 mm, and direct runoff was 199.74 mm, the groundwater recharge rate was determined to be 263.23 mm (19.54% of the total precipitation). Evapotranspiration is greatly affected by land cover and weather, but the change in evapotranspiration is not as large because the land cover does not change significantly in a short period. However, direct runoff is greatly influenced by precipitation, because it includes the accumulated 5-day antecedent precipitation. In particular, very low groundwater recharge can be identified in 1994, 2001, and 2015, which were significantly lower than the annual accumulated precipitation in the study area (Fig. 5B).

In the previous studies, the groundwater recharge rate in the Daejeon Metropolitan City determined by the water table fluctuation and groundwater-level drop curve method was analyzed as 13.9% and 15.15% of the total precipitation, respectively (MOLIT and K-water 2004; Daejeon Metropolitan City 2017). In addition, the recharge rates calculated by groundwater modeling (SWAT (Arnold et al. 2012) and MODFLOW (Harbaugh et al. 2000) and artificial neural networks were reported to be 10.8% and 20.0%, respectively (Hong and Kim 2008; Kim et al. 2019). The groundwater recharge rate of the study area, adapting the water budget method, was estimated as 19.54% of the total precipitation. Groundwater recharge occurs mostly from June to September, which is the growing season. However, minimal recharge occurs in other months, and during some periods, recharge hardly occurs owing to excessive evapotranspiration.

## Hydrochemical properties of groundwater and surface water

The Tandongcheon area is a sub-basin of the Gapcheon River watershed. To comprehensively interpret the hydrochemical connectivity of the study area, it is imperative to assess the water quality of the Gapcheon River and the groundwater in the upstream region. Indeed, considering the influence of regional groundwater and pollutants is an important prerequisite for this research. Thus, this study conducted an analysis of water quality data, including particulate matter (SS and COD), dissolved nutrients (nitrate),

and the total amount of ions (EC) from 2015 to 2021. The data were obtained from (WEIS, 2022) (Fig. 6). The nitrate ( $\text{NO}_3^-$ ) concentration of Gapcheon River achieves drinking water quality standards of Korea (10 mg/L of  $\text{NO}_3^-$ -N, namely 44.3 mg/L of  $\text{NO}_3^-$ ) during the study period (KLIC 2022). As shown in Fig. 6, the SS and EC value also gradually increased to the downstream, but these indices still satisfied the water quality level of the living environmental standards of Korea (within 25 mg/L as very good grade, KLIC 2022). The water qualities of the upper (N1), middle (N2), and lower (N3) streams located in Fig. 1A were maintained very good to normal grade. On the other hand, the COD value showed spatial differences and annual variations, especially downstream, where COD values ranged from marginal to poor grade (KLIC 2022). The observed increase in COD is thought to be influenced by urban anthropogenic inputs, such as domestic sewage or effluence from wastewater treatment plants (WWTP) in Daejeon city (Hur et al. 2008; Hur and Cho 2012). Lee et al. (2006) reported that the main pollutants of Gapcheon River were untreated sewage effluence and discharged water from WWTP, and the COD was 1.9 times higher than the BOD.

The field measurements and ion concentration data of each sampling point are shown in Table 3. The average water temperature of the surface water during the study period was measured to be 22.0 °C, but the surface water temperature at the source of the watershed (S1) was measured relatively low at 17.0 °C. The average water temperature of groundwater was 17.8 °C, showing the average temperature difference of approximately 4.2 °C compared to the surface water. Some of the groundwater (G3, G4, and G7) showed a high-water temperature of approximately 20 °C, and it is considered that the water temperature was high, because the effect of stagnant water remained in the well and because the well was located in the neighborhood parks and was not actively used for a long time. In particular, the EC and total dissolved solids (TDS) levels in the groundwater from the G4 well were the highest among the samples with 1111  $\mu\text{S}/\text{cm}$  and 387 mg/L, respectively. The DO of the G9 and G11 points was 0.24 and 2.12 mg/L, respectively, which was significantly lower than the average DO value of the other groundwater wells, which was 6.69 mg/L. The wells designated for public research purposes, have a depth of approximately 150 m, and are situated on the left (G10) and right (G9) sides of the Tandongcheon.

The Durov diagram is useful for presenting the evolution or mixing trend of the hydrochemical reaction due to the distribution of cations, anions, pH, and TDS values (Durov 1948). Under hydrochemical equilibrium conditions, the groundwater system was verified through measured ionic

**Fig. 6** Water quality diagram from 2015 to 2021 in Gapcheon River

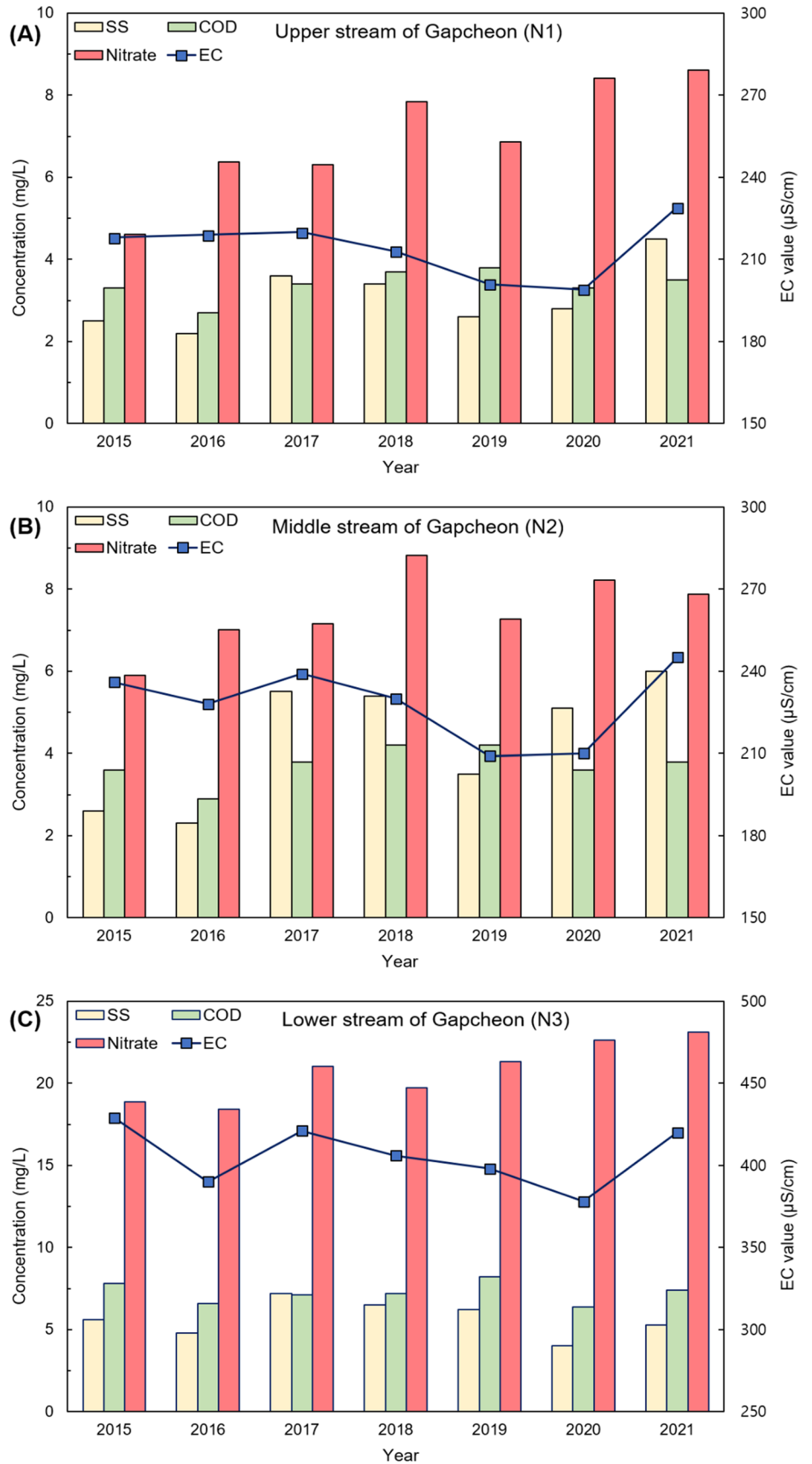


**Table 3** Field measured data and ion analysis results from selected wells and stream points in 2021

Well depth	Temp	DO	EC	pH	Ca	Mg	Na	K	Fe	Mn	SiO <sub>2</sub>	Sr	HCO <sub>3</sub>	F	Cl	NO <sub>2</sub>	NO <sub>3</sub>	SO <sub>4</sub>	TDS	
ID	m	BSL*	°C	mg/L	µS/cm	mg/L	mg/L	mg/L	mg/L	mg/L	mg/L	mg/L	mg/L	mg/L	mg/L	mg/L	mg/L	mg/L	mg/L	mg/L
R1		6.80	9.90	28.74	5.70	1.52	0.217	0.511	0.41	0.100	0.100	0.064	0.100	3.76	0.020	1.35	BDL	3.51	2.71	14.4
R2		20.9	10.2	32.9	5.91	0.45	0.106	0.721	0.32	BDL**	BDL	BDL	BDL	4.15	BDL	0.21	BDL	1.95	1.07	8.86
R3		22.6	9.30	14.0	6.16	0.00	0.039	0.438	0.24	BDL	BDL	BDL	BDL	4.52	BDL	0.22	BDL	2.04	BDL	8.80
S1		17.0	8.25	230	7.14	24.1	4.78	14.3	2.87	0.145	0.115	29.9	0.172	105	0.236	12.5	BDL	4.86	9.28	208
S2		24.5	6.83	182	7.06	18.0	2.53	9.55	2.32	0.017	0.137	9.93	0.126	70.7	0.085	14.4	0.197	4.16	6.02	138
S3		24.6	6.77	97.6	7.09	9.24	1.00	5.34	1.93	0.044	0.102	3.46	0.054	35.5	0.184	8.49	0.170	4.40	4.59	56.0
G1	215	16.2	6.13	886	6.40	42.6	8.06	24.3	4.04	BDL	0.005	24.6	0.428	109	0.162	47.6	BDL	6.36	36.0	319
G2	150	15.6	4.24	798	6.47	40.3	9.86	23.2	1.46	BDL	0.034	41.2	0.412	121	0.523	32.6	BDL	15.6	37.8	324
G3	100	22.4	8.87	459	6.43	20.8	2.65	17.1	1.17	BDL	BDL	38.9	0.310	49.4	BDL	22.6	BDL	22.0	6.38	197
G4	100	19.6	9.18	1111	6.47	51.9	17.1	26.0	1.85	BDL	0.001	49.7	0.447	150	0.263	66.3	BDL	8.93	14.7	387
G5	100	16.4	9.21	343	6.62	35.8	3.98	22.5	1.42	BDL	BDL	37.8	0.443	77.1	BDL	40.5	BDL	23.9	20.7	264
G6	200	18.2	6.83	155	6.78	15.8	3.06	7.45	2.51	BDL	BDL	1.90	0.090	42.8	0.098	19.2	BDL	4.49	11.0	108
G7	110	24.5	6.24	203	6.47	18.7	4.22	13.9	1.26	BDL	BDL	36.4	0.166	67.0	0.253	8.13	BDL	14.8	12.3	193
G8	152	18.2	8.63	550	6.19	57.6	7.48	2.85	1.90	BDL	BDL	43.1	0.916	91.4	0.086	81.4	BDL	38.3	BDL	205
G9	151	16.3	0.24	632	6.08	30.6	5.15	18.4	1.78	0.001	2.355	29.2	0.295	119	0.248	26.6	BDL	BDL	12.8	246
G10	150	15.8	4.57	830	6.22	35.0	3.37	34.0	1.89	0.007	0.007	29.4	0.321	85.4	0.263	64.5	0.686	8.77	14.8	105
G11	180	15.9	2.12	583	7.13	32.5	2.43	14.9	1.06	0.004	0.003	29.7	0.104	114	0.359	16.5	BDL	BDL	BDL	77.6
G12	300	16.4	3.50	745	7.38	57.8	3.42	15.2	1.10	BDL	BDL	34.2	0.249	167	0.240	25.2	BDL	4.50	10.1	319
G13	70	16.6	6.23	344	6.20	23.5	0.575	10.8	0.59	0.005	0.003	27.9	0.136	80.5	1.107	6.07	BDL	3.01	6.60	161
G14	200	17.4	6.64	273	6.77	25.6	2.48	22.3	1.16	BDL	BDL	27.4	0.309	75.1	0.640	21.1	BDL	9.80	23.6	209

\*BSL below surface level  
 \*\*\*BDL below detection limit of each element

**Fig. 7** The Durov diagram of the samples

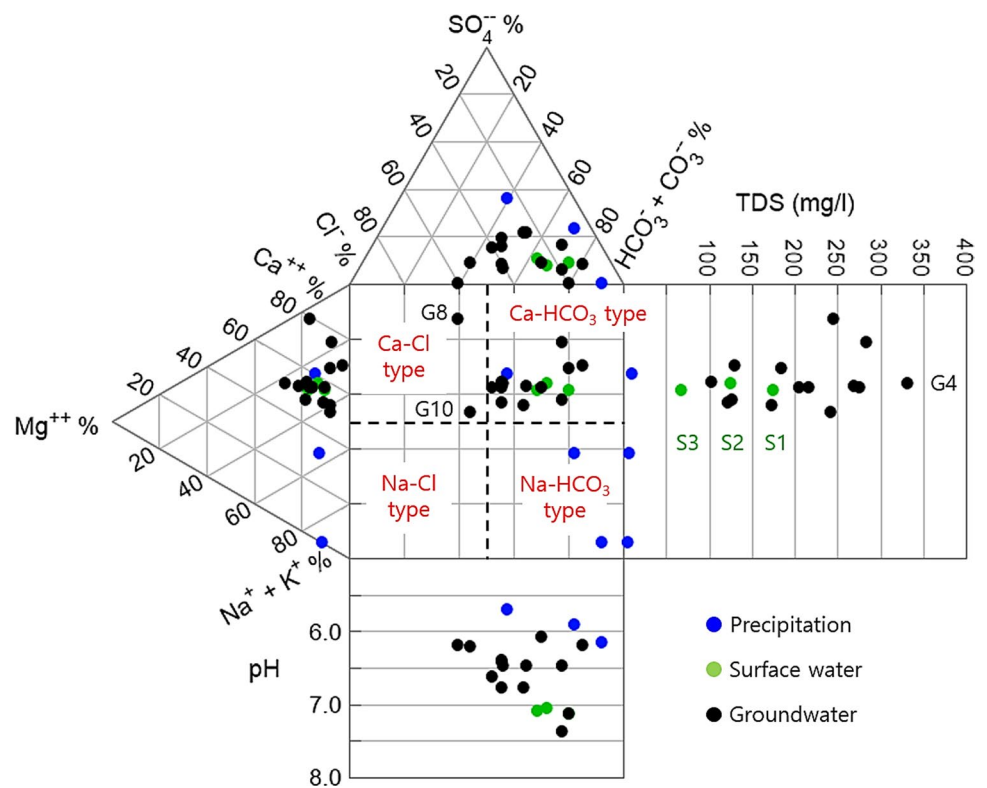
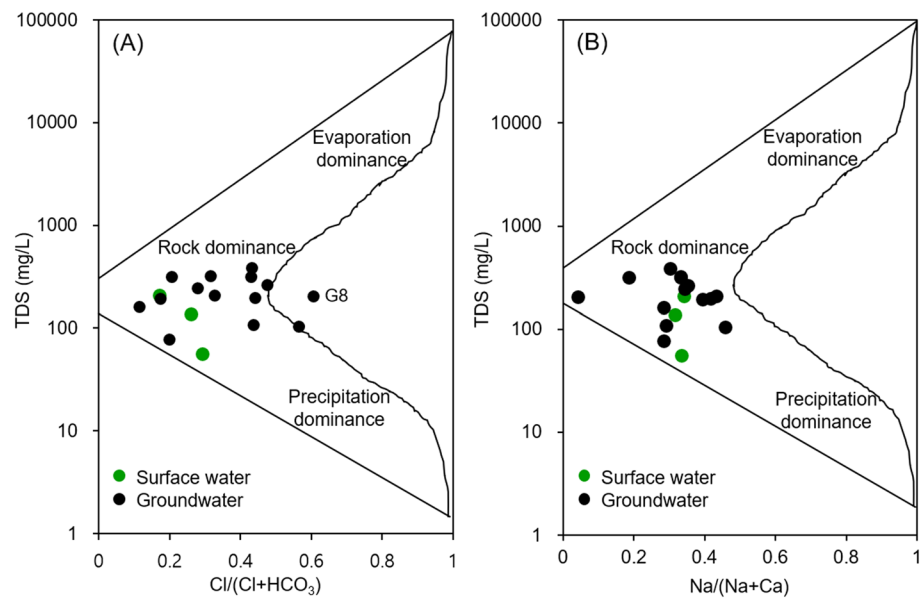


**Fig. 8** Gibbs diagrams for **A** anions versus TDS values, and **B** cations versus TDS values



compositions and field data (pH) plotted on a Durov diagram. As shown in Fig. 7, groundwater (black symbol) and surface water (green symbol) are classified as  $Ca-HCO_3$  type. Precipitation, namely rainwater (blue symbol) collected in March 2021, had the  $Ca-HCO_3$  type, but other

precipitation collected in June 2021 had the  $Na-HCO_3$  type. During the study period, the collected precipitation samples showed TDS values ranging from 8.80 to 14.4 mg/L. The average TDS value of groundwater was measured at 223 mg/L, whereas surface water exhibited a relatively

lower measurement of 134 mg/L. The EC value of the surface water was observed to gradually decrease as it flowed downstream. Yin and Seo (2013) reported that the upstream of Tandongcheon is affected by neighboring military installations and sewage treatment facilities. However, water quality gradually improves as it flows toward the middle and lower sections, attributed to natural purification processes.

In Fig. 7, the G8 and G10 samples showed a Ca-Cl type with a slightly high concentration of Cl<sup>-</sup>, which is typical conservative in water systems. Choi et al. (2020) reported on the G10 sample that had been impacted by amount of NaCl from surface management of the sports ground. The G8 well is situated at the midstream of the watershed and is surrounded by commercial and residential facilities. Notably, the groundwater from the G8 well is consistently pumped four times a day for 30 min each time, except during the winter season. Therefore, the elevated field measured values (temperature and DO) and ion concentrations (EC, Cl<sup>-</sup>, and NO<sub>3</sub><sup>-</sup>, indicating pollution influence) observed in the G8 well are attributed to the inflow of contaminants caused by long-term drainage.

In Fig. 8, the Gibbs diagram is presented to identify the factors influencing the hydrochemistry in the study area, including aquifer lithology, amount of precipitation, and rate of evaporation. The related equation to draw the Gibbs diagram with meq/L units is as follows (Gibbs and McIntyre 1970):

$$I. \text{ Gibbs ratio for anion} = \text{Cl}^- / (\text{Cl}^- + \text{HCO}_3^-), \quad (9)$$

$$II. \text{ Gibbs ratio for cation} = \text{Na}^+ / (\text{Na}^+ + \text{Ca}^{2+}). \quad (10)$$

Most of the water samples plot in rock-weathering dominance, and the G8 sample in Fig. 8A shows higher Cl<sup>-</sup> concentrations than the reference boundary of the river water, but it can occur in nature.

There are many forests and small grains in the upper area, including the boundary of the Tandongcheon sub-watershed area (16.0% of land usage), while urban districts and public areas are located downstream (9.66% of land usage). Anthropogenic pollutants can be introduced into the groundwater and the surface water; thus, this study tried to identify the influence of human activity using Cl<sup>-</sup> and NO<sub>3</sub><sup>-</sup> as contamination indicators. Figure 9A shows that 4 groundwater samples (G7, G11, G12, and G13) and 2 surface water samples (S1 and S2) were classified by ionic composition with a mountain area, whereas the wells that collected the G1, G3, G5, G6, G8, and G10 samples were affected by the domestic area (Yun et al. 2003). This corresponds to approximately 35.3% of the total surface water and groundwater samples in this study area, and the surface water clearly reflects the hydrochemical characteristics of the mountain area.

The background levels of Cl<sup>-</sup> and NO<sub>3</sub><sup>-</sup> in groundwater were reported to be 10–20 mg/L and 3–6 mg/L, respectively, because these components can increase due to excessive fertilizer usage and the penetration of domestic sewage or wastewater (Panno et al. 2006; Kim et al. 2015). Madison and Brunett (1985) reported a background concentration in groundwater of approximately 13.3 mg/L; thus, Fig. 9B shows the anthropogenically influenced water among the samples from the study area. Based on the reference line of the contamination indicator (Madison and Brunett 1985; Panno et al. 2006; Kim et al. 2015), the groundwater that was regarded to be affected by fertilizers or manure constituted approximately 17.6% of the total surface water and groundwater samples. The wells that collected the G2, G5, and G8 samples were located in the vicinity of residential apartment buildings. Additionally, the G2 and G5 wells were situated in small parks with bare ground. The ion composition of these two samples appeared to be influenced by fertilizers or manures, but the contamination level did not exceed the drinking water quality standards in Korea (KLIC 2022). The NO<sub>3</sub><sup>-</sup> level of the G8 was measured at 38.28 mg/L which is close to the drinking water quality standard (about

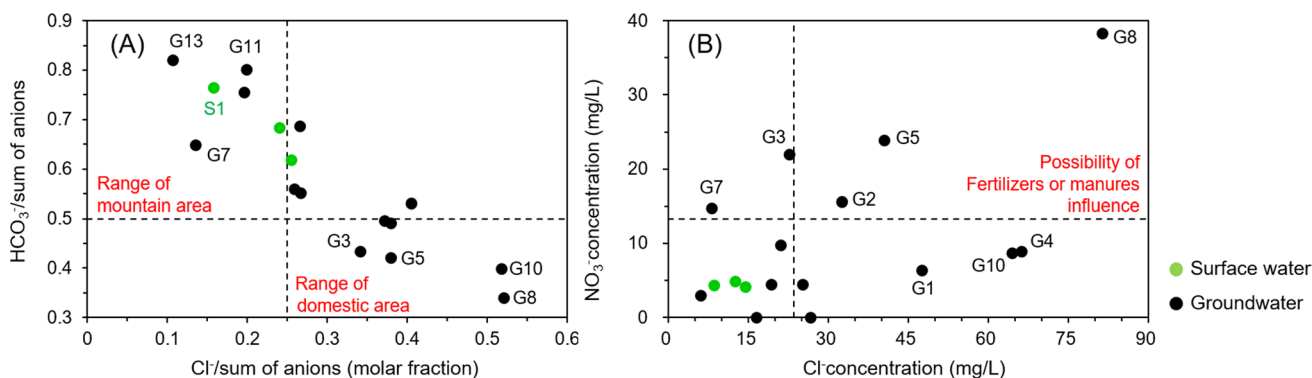
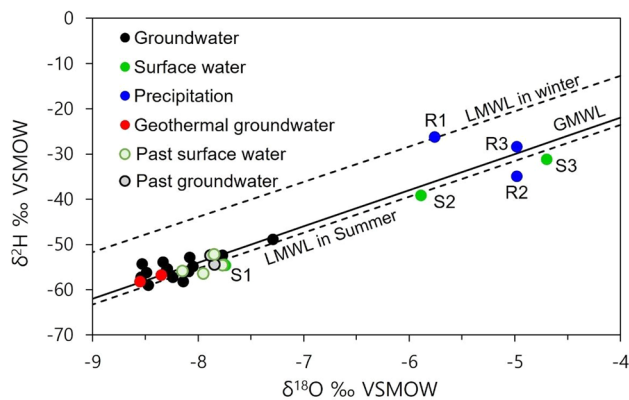


Fig. 9 A Classification of groundwater and surface water with anion references and B verification of anthropogenic influences

**Table 4** Isotope analysis data of oxygen, hydrogen, and strontium from 2015 to 2021

ID	Date	$\delta^{18}\text{O}$ ‰ VSMOW	$\delta^2\text{H}$	$^{87}\text{Sr}/^{86}\text{Sr}$	2 $\sigma$ SE	I/Sr mg/L <sup>-1</sup>	References
R1	Mar. 2021	- 5.76	- 26.28	-	-	10.0	This study
R2	Jun. 2021	- 4.98	- 34.92	-	-		
R3		- 4.98	- 28.38	-	-		
S1		- 7.75	- 54.39	0.717086	0.000009	5.83	Choi et al. (2020)
S2		- 5.89	- 39.19	0.715419	0.000010	7.95	
S3		- 4.70	- 31.20	0.715308	0.000009	18.6	
G1		- 8.08	- 52.84	0.715267	0.000011	2.33	
G2		- 7.29	- 48.90	0.715466	0.000010	2.43	
G3		- 8.33	- 53.89	0.715693	0.000009	3.23	
G4		- 7.77	- 52.39	0.715966	0.000009	2.24	
G5		- 8.09	- 56.01	0.716831	0.000009	2.26	
G6		- 8.05	- 54.88	0.720099	0.000009	11.1	
G7		- 8.47	- 58.97	0.717384	0.000010	6.03	
G8		- 8.14	- 58.17	0.715557	0.000009	1.09	
G9		- 8.53	- 54.28	0.714977	0.000009	3.39	
G10		- 8.30	- 55.83	0.716154	0.000009	3.12	
G11		- 8.29	- 55.44	0.716657	0.000009	9.59	
G12		- 8.49	- 56.25	0.715885	0.000008	4.01	
G13		- 8.54	- 57.27	0.716145	0.000009	7.37	
G14		- 8.24	- 57.21	0.716380	0.000008	3.24	
S2-1	Jan. 2019	- 7.95	- 56.5	0.716034	0.000009	4.47	Choi et al. (2020)
S2-2	Feb. 2019	- 8.14	- 55.9	0.716049	0.000009	4.48	
S3-1	Apr. 2015	- 7.86	- 52.4	0.716733	0.000009	7.85	Choi (2017)
S3-2	May 2015	- 7.74	- 54.6	0.716857	0.000009	6.82	
G3-1	Apr. 2015	- 7.88	- 52.5	0.715550	0.000008	1.79	
G3-2	May 2015	- 7.85	- 54.2	0.716023	0.000009	1.74	
T3-1	Apr. 2015	- 8.35	- 56.8	0.715677	0.000009	3.32	
T3-2	May 2015	- 8.55	- 58.2	0.716016	0.000009	7.05	



**Fig. 10** The  $\delta^{18}\text{O}$  and  $\delta^2\text{H}$  pairs of various water samples obtained from 2015 to 2021

44.3 mg/L of  $\text{NO}_3^-$ ). Therefore, it is deemed essential to conduct continuous monitoring to prevent nitrate contamination and ensure water quality safety. On the other hand, the surface water samples were found to be significantly less influenced by anthropogenic pollutants compared to the groundwater samples.

## Interpretation of isotopic composition

### Oxygen and hydrogen isotopes

The oxygen ( $\delta^{18}\text{O}$ ) and hydrogen ( $\delta^2\text{H}$ ) isotopic compositions of water samples can be used to estimate the recharge rate, evaporation, groundwater, and surface water mixing (Bhat and Jeelani 2018; Ma et al. 2019). This study utilized eight previously collected samples (four surface waters, two groundwaters, and two geothermal groundwaters) to compare the temporal changes in isotope compositions (Table 4). The groundwater, surface water, and geothermal groundwater samples were collected in April and May 2015, with two samples of each type (Choi 2017). Additionally, two surface water samples were collected in January and February 2019 (Choi et al. 2020). The groundwater and geothermal groundwater samples were collected from the hot spring area, situated between the G1 and G6 points, as part of this monitoring campaign. Surface water in 2015 was collected from the downstream section of Gapcheon (see Appendix for more details), while the surface water in 2019 was collected at the same point as S2 of this monitoring campaign (see Fig. 4). The mean and standard deviation values of the  $\delta^{18}\text{O}$ - $\delta^2\text{H}$  pair from groundwater collected in 2021 were  $-8.13 \pm 0.313\text{‰}$  for  $\delta^{18}\text{O}$  and  $-55.2 \pm 2.33\text{‰}$  for  $\delta^2\text{H}$  (Table 4).

The  $\delta^{18}\text{O}$ - $\delta^2\text{H}$  pairs of the Global Meteoric Water Line (GMWL) and the Local Meteoric Water Line (LMWL) of South Korea using precipitation and surface water have been reported using the following equation (Craig 1961; Lee 1999):

$$\text{Global meteoric water line : } \delta^2\text{H} = 8\delta^{18}\text{O} + 10, \quad (11)$$

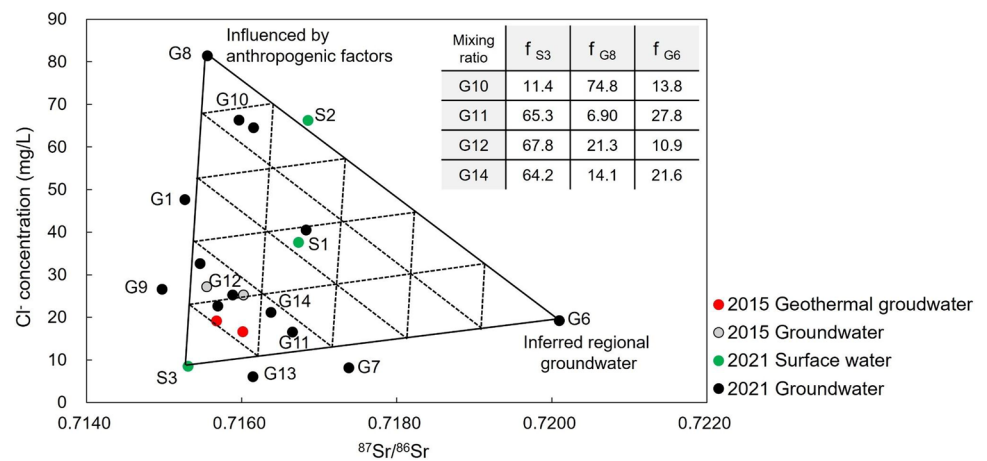
$$\text{Regression line in summer, Korea : } \delta^2\text{H} = 7.93\delta^{18}\text{O} + 8.11, \quad (12)$$

$$\text{Regression line in winter, Korea : } \delta^2\text{H} = 7.79\delta^{18}\text{O} + 18.39. \quad (13)$$

The LMWL reference of Lee (1999) is based on the precipitation and surface water data from the Daejeon (study area) and Seoul (located in the northern part of the study area). South Korea has five official stations of the global network of isotopes in precipitation from the International Atomic Energy Agency: Pohang (1961–1976), Cheongju (1998–2016), Hongseong (2018–present), Busan (2019–present), and Jeju (2020–present). The stations currently in operation, Hongseong, Busan, and Jeju, may require additional data to establish representativeness. In comparison, Jung et al. (2019) reported the seasonal LMWL of Mt. Gyeryong, located approximately 12 km west of the study area:  $\delta^2\text{H} = 7.98 \delta^{18}\text{O} + 9.28$  ( $n = 69$ ,  $R^2 = 0.98$ ) for summer (June–September) precipitation, and  $\delta^2\text{H} = 7.16 \delta^{18}\text{O} + 17.97$  ( $n = 66$ ,  $R^2 = 0.87$ ) for winter (November to February). It seemed similar LMWL to the reference data of Lee (1999). Throughout this study period, the precipitation collected in March (R1) is plotted on the LMWL for winter, while the summer precipitation samples (R2 and R3, collected in June) are plotted on the LMWL for summer. Furthermore, all the groundwater and surface water samples are distributed along the GMWL of Craig (1961). This indicates that most water samples in this area originated from meteoric water, with no significant differences observed in their isotope composition despite temporal variations (see Fig. 10).

The S1 sample has a similar  $\delta^{18}\text{O}$ - $\delta^2\text{H}$  composition to that of most groundwater samples in the study area, but the S2 and S3 samples have significantly enriched values reflecting the influence of precipitation. The isotope values of S2 and R1–R3, which were collected at similar locations in the Tandongcheon sub-watershed, are nearly identical. Moreover, the site with the lowest altitude, S3, exhibits the most enriched isotope composition. This difference is attributed to the altitude effect, wherein precipitation with a heavier isotopic composition is observed at lower altitudes (Clark and Fritz 1997). Therefore, it is inferred that most of the groundwater in the study area and the surface water S1 have been recharged at a higher elevation than the study area, leading to a more depleted isotope composition.

**Fig. 11** The  $\text{Cl}^-$  concentration versus  $^{87}\text{Sr}/^{86}\text{Sr}$  ratio diagram and calculated endmember mixing results. Dashed lines represent mixing ratios among the three endmembers at 20% intervals



### Sr isotopic compositions

Strontium (Sr) concentration in the water system can be affected by natural and anthropogenic sources: interaction between percolated rainwater and Sr-bearing minerals such as calcite or plagioclase in the aquifer is the primary natural process (Lee et al. 2011). In comparison, the anthropogenic influence from fertilizers and deicing salts can affect the hydrochemical composition of the water system (Négré et al. 2004). By contrast, Sr isotopic composition ( $^{87}\text{Sr}/^{86}\text{Sr}$  ratio) is affected by the Rb/Sr ratio due to the age of lithologic materials, and variations in Sr concentration do not impact Sr isotope fractionation (Négré et al. 2004; Lee et al. 2011; Kim et al. 2020). Based on it, the  $^{87}\text{Sr}/^{86}\text{Sr}$  ratio is an effective tracer used to estimate the mixing of water bodies that have undergone various processes (Négré et al. 2004; Kim et al. 2020). The Jurassic granite in this study area has been reported to have  $^{87}\text{Sr}/^{86}\text{Sr}$  ratios ranging from 0.7080 to 0.7216 (Jwa 2004). The bulk deposition of precipitation in Korea has been reported to have  $^{87}\text{Sr}/^{86}\text{Sr}$  ratios ranging from 0.7109 to 0.7128, and this ratio was found to be distributed between 0.7109 and 0.7128 in both the coastal and inland areas of South Korea (Jeon and Chung 2005). Jung et al. (2019) reported that the surface water of lower order streams in the middle and upper zones in the Geum River basin, including the study site, exhibited the influence of groundwater discharge from mountainous areas. The study area, southern region of Yuseong-gu, is characterized by the presence of Okcheon metamorphic rocks, and the  $^{87}\text{Sr}/^{86}\text{Sr}$  ratio of this site has been reported to be notably high, up to 0.8298 (Park and Cheong 1998). It is generally reported that old metamorphic rocks exhibit higher  $^{87}\text{Sr}/^{86}\text{Sr}$  ratios compared to relatively young granite due to the extended decay of Rb (rubidium) for a long time in the metamorphic rock (Bataille and Bowen 2012). Hence, it is inferred that the groundwater flowing through the region where metamorphic

rocks are prevalent could potentially possess elevated  $^{87}\text{Sr}/^{86}\text{Sr}$  ratios because of interactions with the minerals in the bedrock. Site G6 is located at the convergence of Gapcheon and its tributary stream Yuseongcheon, in a hot spring area. Despite its location in a hot spring area and its well depth of 200 m, the groundwater at site G6 was observed to have a similar  $^{87}\text{Sr}/^{86}\text{Sr}$  ratio to that of other groundwater sources in the study site.

### EMMA at Tandongcheon sub-watershed

To comprehend the hydrological cycle of the Tandongcheon sub-watershed, two distinct indicators as a natural tracer were utilized to distinguish the endmembers: the strontium isotope ratio ( $^{87}\text{Sr}/^{86}\text{Sr}$ ) and  $\text{Cl}^-$  concentration. These variables were selected for their conservative properties to determine the mixing ratios of different water bodies; thus, many researchers have applied these components applied in the Tandongcheon sub-watershed (Lee et al. 2011; Choi et al. 2020; He et al. 2022). Figure 11 illustrates the possibility of three endmember components which are S3, G6, and G8 samples to analyze mixing processes at this site. We did not analyze the surface water acquired between 2015 and 2019 due to its susceptibility to external influences. Because its susceptibility to external influences, such as seasonal variations and human activities, can cause relatively significant changes in water quality to surface water, especially  $\text{Cl}^-$  concentration (Choi 2017).

The endmember G6 exhibits a relatively high  $^{87}\text{Sr}/^{86}\text{Sr}$  ratio of 0.7201 compared to the other water samples, which were collected from wells with depths of 200 m. It is expected that regional groundwater undergoes interaction with metamorphic rocks and migrates along geological lineaments, potentially affecting the G6 aquifer. In comparison, most of the water samples including geothermal groundwater



in the study area exhibit a narrow range of  $^{87}\text{Sr}/^{86}\text{Sr}$  ratio from 0.7150 to 0.7174, suggesting that temporary similar water–rock interaction occurred in this area. The endmember G8 has the highest both  $\text{NO}_3^-$  and  $\text{Cl}^-$  concentration in the study area due to the influence of anthropogenic contamination. Despite this influence, the concentrations remain within the drinking water quality standard of Korea (KLIC 2022). As discussed earlier, the continuous pumping of the G8 sampling site groundwater appears to accelerate contamination introduced from surrounding residential and commercial facilities with the groundwater movement. The endmember S3 sample presents the lowest  $\text{Cl}^-$  concentration and  $^{87}\text{Sr}/^{86}\text{Sr}$  ratio in Fig. 11. The  $\delta^{18}\text{O}$ – $\delta^2\text{H}$  composition and the TDS value at this site suggest that it largely reflects the original quality of surface water from the recharges water nearby mountainous region with minimal anthropogenic pollution influence.

The results of contribution ratio by each endmember are shown as the table in Fig. 11. Groundwater at the G10 site showed water quality characteristics affected by anthropogenic inputs, and thus, this site was calculated that the mixing ratio of G8 was quite high in three-component mixing. Excluding G10, other points of groundwater sampling in the Tandongcheon sub-watershed were mainly affected by surface water (S3) around 65% mixing ratio (see the table in the Fig. 11). It can be inferred that the quality of groundwater in the Tandongcheon sub-watershed is primarily influenced by two factors: local precipitation recharge and water–rock interaction with the bedrock.

## Conclusions

This study demonstrated the groundwater recharge estimation and mixing characteristics of mountainous surface water and groundwater using natural tracers. The water budget methods (FAO-56 PM and SCS-CN methods) were applied to calculate evapotranspiration and direct runoff with precipitation data to estimate recharge rate. Calculated recharge rate of the groundwater area was determined to be 263.23 mm, accounting for 19.54% of the total precipitation.

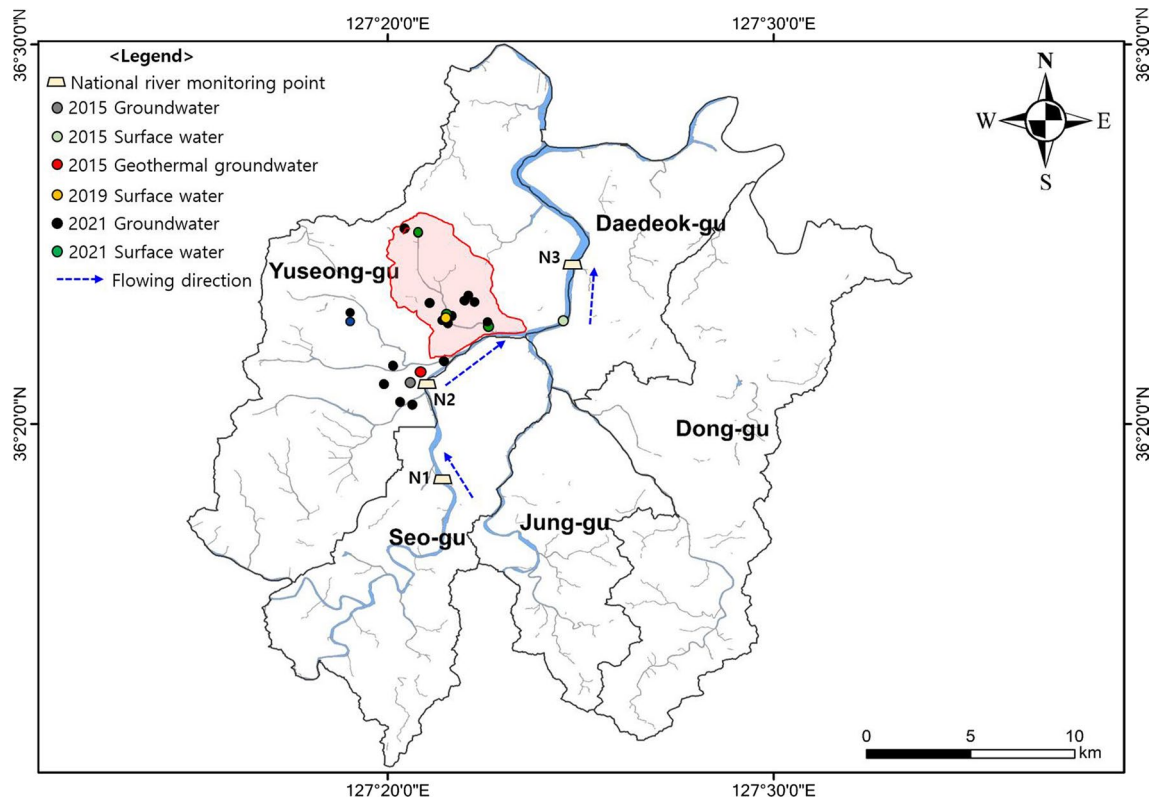
The land-use properties are distributed in the order of forest, public area, small grain area, and their impact is

discernibly manifested in the hydrochemical characteristics within the study area. Approximately 35% of the whole samples exhibited characteristic of mountainous regions, while 18% of the groundwater samples were classified to affect by anthropogenic inputs such as domestic sewage or military effluences. The  $\delta^{18}\text{O}$ – $\delta^2\text{H}$  composition revealed an altitude effect in the surface water, which gives the inference that the groundwater was recharged at a higher altitude region. Moreover, the samples including surface water, groundwater, and geothermal groundwater exhibit a narrow range of  $^{87}\text{Sr}/^{86}\text{Sr}$  ratio from 0.7150 to 0.7174, suggesting that temporary similar water–rock interaction occurred at this region. The higher  $^{87}\text{Sr}/^{86}\text{Sr}$  ratio of G6 which was gained external point of the Tandongcheon watershed boundary is attributed to the influence of mixing from Gapcheon River, as well as the regional pathway of the groundwater.

The application of the three-component endmember mixing analysis revealed that local groundwater is predominantly influenced by surface water (S3), indicating a close interrelationship between surface water and groundwater in mountain hydrology. However, it is noteworthy that anthropogenic factors have been associated with the increase in chloride ( $\text{Cl}^-$ ) concentration in both surface water and groundwater within the public area. This study provides insights into groundwater recharge and the connectivity of water bodies in the mountainous watershed through the use of natural tracers. Indeed, it is possible that both surface water and groundwater may be simultaneously affected in the case of pollution incidents, and the degradation of water quality in tributaries potentially has an effect on the higher order stream. The approach employed in this study can contribute to enhancing comprehension of sustainable water resources' management, encompassing both local and regional scales.

## Appendix 1

Sampling points of groundwater, thermal groundwater, and surface water. The spots of N1–N3 show National River monitoring points, and the sampling points of groundwater and surface water in 2015 are also presented.



**Acknowledgements** This work was supported by the Basic Research Project (22-3411) of the Korea Institute of Geoscience and Mineral Resources (KIGAM) funded by the Ministry of Science and ICT (MSIT). The authors would like to thank the Hyosik Seo and Dr. Dong-Chan Koh for their help on data acquisition and sample analysis.

**Author contributions** HC: conceptualization, methodology, data curation, formal analysis, investigation, and writing—original draft; CML: data collection, validation, formal analysis, and writing—draft; HJJ: data collection and writing—draft; BOS: data collection, data curation, validation, formal analysis, and writing—review and editing.

**Funding** This research was supported by the Basic Research Project of Korea Institute of Geoscience and Mineral Resources (KIGAM).

**Data availability** The manuscript contains all the data and explanations.

## Declarations

**Conflict of interest** No potential conflict of interest was reported by the authors.

**Open Access** This article is licensed under a Creative Commons Attribution 4.0 International License, which permits use, sharing, adaptation, distribution and reproduction in any medium or format, as long as you give appropriate credit to the original author(s) and the source, provide a link to the Creative Commons licence, and indicate if changes were made. The images or other third party material in this article are included in the article's Creative Commons licence, unless indicated otherwise in a credit line to the material. If material is not included in

the article's Creative Commons licence and your intended use is not permitted by statutory regulation or exceeds the permitted use, you will need to obtain permission directly from the copyright holder. To view a copy of this licence, visit <http://creativecommons.org/licenses/by/4.0/>.

## References

- Aboukhaled A, Alfaro A, Smith M (1982) In Food and Agriculture Organization of the United Nations (FAO) irrigation and drainage paper 39. FAO Publication, Rome
- Agriinfo (2018) Watershed Classification in Watershed Management Including Surveying, My Agriculture Information Bank. Available from: <https://agriinfo.in/classification-of-watershed-75/>. Accessed 25 July 2023.
- Allen, RG, Pereira LS, Raes D, Smith M (1998) Crop evapotranspiration-Guidelines for computing crop water requirements-FAO Irrigation and drainage paper 56. Fao, Rome, 300(9), D05109
- Anuraga TS, Ruiz L, Kumar MM, Sekhar M, Leijnse A (2006) Estimating groundwater recharge using land use and soil data: A case study in South India. *Agric Water Manag* 84:65–76
- Arnold JG, Moriasi DN, Gassman PW, Abbaspour KC, White MJ, Srinivasan R, Santhi C, Harmel RD, van Griensven A, Van Liew MW, Kannan N, Jha MK (2012) SWAT: Model use, calibration, and validation, Michigan, pp. 1491–1508.
- Bataille CP, Bowen GJ (2012) Mapping  $^{87}\text{Sr}/^{86}\text{Sr}$  variations in bedrock and water for large scale provenance studies. *Chem Geol* 304:39–52

- Bhat NA, Jeelani G (2018) Quantification of groundwater–surface water interactions using environmental isotopes: a case study of Bringi Watershed, Kashmir Himalayas. *India J Earth Syst Sci* 127:63
- Choi H (2017) Spatio-temporal variations of hydrogeochemistry of selected geothermal groundwater and carbonated groundwater in Korea: drawing a baseline for CCS detection monitoring. Dissertation, University of Yonsei
- Choi H, Kim J, Shim BO, Kim DH (2020) Characterization of aquifer hydrochemistry from the operation of a shallow geothermal system. *Water* 12:1377
- Clark ID, Fritz P (1997) *Environmental isotopes in hydrogeology*. CRC Press, Florida
- Craig H (1961) Isotopic variations in meteoric waters. *Science* 133:1702–1703
- Daejeon Metropolitan city (2017) Summary Report of Groundwater Management Plan in Daejeon Metropolitan City. Daejeon Metropolitan City, 48
- Durov S (1948) Classification of natural waters and graphic representation of their composition. *Dokl Akad Nauk SSSR* 59(1):87–90
- Gee GW, Hillel D (1988) Groundwater recharge in arid regions: review and critique of estimation methods. *Hydrol Process* 2:255–266
- Gibbs AJ, McIntyre GA (1970) The diagram, a method for comparing sequences: its use with amino acid and nucleotide sequences. *Eur J Biochem* 16:1–11
- Gonzalez R, Ouarda TB, Marpu PR, Allam MM, Eltahir EA, Pearson S (2016) Water budget analysis in arid regions, application to the United Arab Emirates. *Water* 8:415
- Harbaugh AW, Banta ER, Hill MC, McDonald MG (2000) *Modflow-2000, the U.S. geological survey modular ground-water model-user guide to modularization concepts and the ground-water flow process*. Open-file Report, U.S. Geological Survey
- Havril T, Tóth Á, Molson JW, Galsa A, Mádl-Szónyi J (2018) Impacts of predicted climate change on groundwater flow systems: can wetlands disappear due to recharge reduction? *J Hydrol* 563:1169–1180
- He X, Li P, Shi H, Xiao Y, Guo Y, Zhao H (2022) Identifying strontium sources of flowback fluid and groundwater pollution using  $^{87}\text{Sr}/^{86}\text{Sr}$  and geochemical model in Sulige gasfield. *China Chemosphere* 306:135594
- Hong SH, Kim JK (2008) Analysis of Groundwater Use in Kapcheon Basin. *J Korea Water Resour Assoc* 41:463–471 (in Korean with English abstract)
- Hounslow AW (2018) *Water quality data: analysis and interpretation*. CRC Press, Florida. <https://doi.org/10.1201/9780203734117>
- Hur J, Cho J (2012) Prediction of BOD, COD, and total nitrogen concentrations in a typical urban river using a fluorescence excitation-emission matrix with PARAFAC and UV absorption indices. *Sensors* 12(1):972–986
- Hur J, Hwang SJ, Shin JK (2008) Using synchronous fluorescence technique as a water quality monitoring tool for an urban river. *Water Air Soil Pollut* 191(1):231–243
- Hwang J (2013) Occurrence of U-minerals and source of U in groundwater in Daebo granite, Daejeon area. *J Eng Geol* 23:399–407
- IPCC (Intergovernmental Panel on Climate Change) (2021) *Weather and climate extreme events in a changing climate*. In IPCC Sixth Assessment Report. <https://www.ipcc.ch/report/ar6/wg1/chapter/chapter-11/>. Accessed 1 July 2023
- Jang S, Hamm SY, Yoon H, Kim GB, Park JH, Kim M (2015) Predicting long-term change of groundwater level with regional climate model in South Korea. *Geosci J* 19:503–513
- Jang Y, Son B, Chu S, Lim B (2019) Characteristics and management plan of water quality at the water pollution deterioration area of the upper stream of Gapcheon. *J Korean Soc Water Environ* 35(5):399–408 (in Korean with English abstract)
- Jeon SR, Chung JI (2005) The Sr and Pb isotopic and geochemical properties of the atmospheric bulk deposition of Jeonju, Gunsan, and Namwon areas. *Econ Environ Geol* 38(4):463–479
- Jo HJ, Cheong ACS, Yi K, Li XH (2018) Juxtaposition of allochthonous terranes in the central Korean Peninsula: Evidence from zircon U–Pb ages and O–Hf isotopes in Jurassic granitoids. *Chem Geol* 484:136–147
- Jo HJ, Cheong ACS, Yi K, Li XH (2021) Determination of Sr–Nd–Pb isotopic ratios of rock reference materials using column separation techniques and TIMS. *Separations* 8:213
- Jung YY, Koh DC, Yoon YY, Kwon HI, Heo J, Ha K, Yun ST (2019) Using stable isotopes and tritium to delineate groundwater flow systems and their relationship to streams in the Geum River basin, Korea. *J Hydrol* 573:267–280
- Jwa YJ (2004) Possible source rocks of Mesozoic granites in South Korea: implications for crustal evolution in NE Asia. *Earth Environ Sci Trans R Soc Edinb* 95(1–2):181–198
- Kang Y, Park CS, Park J, Cho D (2018) Spatial differences in the heavy precipitation risk intensity in South Korea. *Hum Ecol Risk Assess* 24:1579–1594
- KLIC (Korean Law Information Center) 2022. Act on Environmental Policy of Korea. Available from: <https://www.law.go.kr/LSW/main.html>. Accessed 28 Dec 2022
- Kim KH, Yun ST, Kim HK, Kim JW (2015) Determination of natural backgrounds and thresholds of nitrate in South Korean groundwater using model-based statistical approaches. *J Geochem Explor* 148:196–205
- Kim GB, Hwang CI, Shin HJ, Choi MR (2019) Applicability of groundwater recharge rate estimation method based on artificial neural networks in unmeasured areas. *J Geol Soc Korea* 55:693–701 (in Korean with English abstract)
- Kim J, Choi H, Kim H, Ryu JS, Lee KK (2020) Using isotopes (strontium and radon) and microbial communities to quantify groundwater mixing influenced by anthropogenic factors at riverside area. *J Hydrol* 581:124441
- Lee K, Lee CB (1999) Oxygen and hydrogen isotopic composition of precipitation and river waters in South Korea. *J Geol Soc Korea* 35:73–84 (in Korean with English abstract)
- Lee HS, Hur J, Jeong SA, Hwang SJ, Shin JK (2006) Spatial characterization of water pollution in the urban stream watershed (Gap Stream), Korea. *J Korean Soc Water Quality* 22(5):943–951 (in Korean with English abstract)
- Lee SG, Kim TK, Lee TJ (2011) Strontium isotope geochemistry and its geochemical implication from hot spring waters in South Korea. *J Volcanol Geoth Res* 208(1–2):12–22
- Lee SH, Oh CW, Jung S (2021) Jurassic igneous activity in the Yuseong area on the southern margin of the Gyeonggi Massif, Korean Peninsula, and its implications for the tectonic evolution of northeast Asia during the Jurassic. *Minerals* 11:466
- Ma B, Jin M, Liang X, Li J (2019) Application of environmental tracers for investigation of groundwater mean residence time and aquifer recharge in fault-influenced hydraulic drop alluvium aquifers. *Hydrol Earth Syst Sci* 23(1):427–446
- Manghi F, Mortazavi B, Crother C, Hamdi MR (2009) Estimating regional groundwater recharge using a hydrological budget method. *Water Resour Manage* 23:2475–2489
- Madison RJ, Brunett JO (1985) Overview of the occurrence of nitrate in ground water of the United States, in National Water Summary 1984-Hydrologic Events, Selected Water-Quality Trends, and Ground-Water Resources: U.S. Geological Survey Water-Supply Paper. 2275
- MOLIT (Ministry of Land, Infrastructure and Transport) and K-water (Korea Water Resources Corporation) (2004) Report of Groundwater Basic Survey in Daejeon Metropolitan city. Sejong, MOLIT. 274p

- Munia HA, Guillaume JH, Wada Y, Veldkamp T, Virkki V, Kummu M (2020) Future transboundary water stress and its drivers under climate change: a global study. *Earth's Fut* 8(7):e2019EF001321
- Négrel P, Petelet-Giraud E, Widory D (2004) Strontium isotope geochemistry of alluvial groundwater: a tracer for groundwater resources characterisation. *Hydrol Earth Syst Sci* 8(5):959–972
- NGII (National Geographic Information Institute) (2016) The national atlas of Korea II. Gyeonggi, Korea
- Owuor SO, Butterbach-Bahl K, Guzha AC, Rufino MC, Pelster DE, Díaz-Pinés E, Breuer L (2016) Groundwater recharge rates and surface runoff response to land use and land cover changes in semi-arid environments. *Ecol Process* 5:16
- Panno SV, Hackley KC, Hwang HH, Greenberg SE, Krapac IG, Landsberger S, O'Kelly DJ (2006) Characterization and identification of Na-Cl sources in ground water. *Groundwater* 44(2):176–187
- Park KH, Cheong CS (1998)  $^{87}\text{Sr}/^{86}\text{Sr}$  ratios and ages of the Ogcheon metasedimentary rocks. *J Geol Soc Korea* 34(2):81–93 (in Korean with English abstract)
- Peng TR, Huang CC, Chen JE, Zhan WJ, Chiang LW, Chang LC (2016) Evaluating the relative importance of groundwater recharge sources in a subtropical alluvial plain using tracer-based ternary endmember mixing analysis (EMMA). *Water Resour Manage* 30(11):3861–3878
- Ponce VM, Hawkins RH (1996) Runoff curve number: Has it reached maturity? *J Hydrol Eng* 1(1):11–19
- Scanlon BR, Healy RW, Cook PG (2002) Choosing appropriate techniques for quantifying groundwater recharge. *Hydrogeol J* 10:18–39
- Scanlon BR, Reedy RC, Stonestrom DA, Prudic DE, Dennehy KF (2005) Impact of land use and land cover change on groundwater recharge and quality in the southwestern US. *Glob Change Biol* 11:1577–1593
- Somers LD, McKenzie JM (2020) A review of groundwater in high mountain environments. *Wiley Interdiscip Rev Water* 7(6):e1475
- WEIS (Water Environment Information System) (2022) Water quality monitoring system. Available from: <https://water.nier.go.kr/>. Accessed 30 Dec 2022
- Wu Q, Wang G, Zhang W, Cui H, Zhang W (2016) Estimation of groundwater recharge using tracers and numerical modeling in the north china plain. *Water* 8:353
- Xu CY, Chen D (2005) Comparison of seven models for estimation of evapotranspiration and groundwater recharge using lysimeter measurement data in Germany. *Hydrol Process* 19:3717–3734
- Yifru BA, Chung IM, Kim MG, Chang SW (2022) Augmenting freshwater availability in mountain headwater streams: Assessing the sustainability under baseline and future climate change scenarios. *Int Soil Water Conserv Res* 10(2):293–307
- Yin Z, Seo D (2013) Application of QUAL2K model for Daejeon Tandongcheon, a small urban stream and evaluation of terrace land constructed wetland. *J Korean Soc Environ Eng* 35(3):192–199
- Yun W, Ji SJ, So CS (2003) The hydrochemical and stable isotope characteristics of shallow groundwater near the Gwangju stream. *Econ Environ Geol* 36(6):441–455
- Zou S, Jilili A, Duan W, Maeyer PD, de Voorde TV (2019) Human and natural impacts on the water resources in the Syr Darya River Basin, Central Asia. *Sustain* 11(11):3084

**Publisher's Note** Springer Nature remains neutral with regard to jurisdictional claims in published maps and institutional affiliations.